

Received: 2016.03.18  
Accepted: 2016.04.28  
Published: 2016.07.07

# Experimental Study of Magnetic Multi-Walled Carbon Nanotube-Doxorubicin Conjugate in a Lymph Node Metastatic Model of Breast Cancer

Authors' Contribution:  
Study Design A  
Data Collection B  
Statistical Analysis C  
Data Interpretation D  
Manuscript Preparation E  
Literature Search F  
Funds Collection G

ABCDEF 1 **Jian Ji\***  
ABCDEF 2 **Minfeng Liu\***  
BCDEF 3 **Yue Meng**  
BCDEF 2 **Runqi Liu**  
BCD 2 **Yan Yan**  
BEF 2 **Jianguo Dong**  
BCDE 2 **Zhaoze Guo**  
ABCDEF 2 **Changsheng Ye**

1 Department of Hepatobiliary Breast Surgery, The Fifth Affiliated Hospital of Southern Medical University, Guangzhou, Guangdong, P.R. China  
2 Department of Breast Surgery, Nanfang Hospital, Southern Medical University, Guangzhou, Guangdong, P.R. China  
3 Department of Orthopaedics, The Fifth Affiliated Hospital of Southern Medical University, Guangzhou, Guangdong, P.R. China

\* Jian Ji and Minfeng Liu is the co-first author

**Corresponding Authors:**

Minfeng Liu, e-mail: [matthewliu007@163.com](mailto:matthewliu007@163.com), Changsheng Ye, e-mail: [yechangsheng\\_001@163.com](mailto:yechangsheng_001@163.com)

**Source of support:**

This work was supported by the Science and Technology Planning Project of Guangdong Province (2012B010300013)

**Background:** The lymphatic system plays a significant role in the defense of a subject against breast cancer and is one of the major pathways for the metastasis of breast cancer. To improve the prognosis, many means, including surgery, radiotherapy, and chemotherapy, have been used. However, the combination of all these modalities has limited efficacy. Lymph nodes, therefore, have become an exceptionally potential target organ in cancer chemotherapy.

**Material/Methods:** A lymph node metastatic model of breast cancer was established in BALB/c mice. Magnetic multi-walled carbon nanotube carrier with good adsorption and lymph node-targeting capacity was prepared and conjugated with doxorubicin to make the magnetic multi-walled carbon nanotube-doxorubicin suspension. Dispersions of doxorubicin, magnetic multi-walled carbon nanotube-doxorubicin, and magnetic multi-walled carbon nanotube were injected into lymph node metastatic mice to compare their inhibitory effects on tumor cells *in vivo*. Inhibition of these dispersions on EMT-6 breast cancer cells was detected via MTT assay *in vitro*.

**Results:** Although no significant difference was found between the effects of doxorubicin and magnetic multi-walled carbon nanotube-doxorubicin with the same concentration of doxorubicin on EMT-6 breast cancer cells *in vitro*, in terms of sizes of metastatic lymph nodes and xenograft tumors, apoptosis in metastatic lymph nodes, and adverse reactions, the magnetic multi-walled carbon nanotube-doxorubicin group differed significantly from the other groups.

**Conclusions:** The magnetic multi-walled carbon nanotube-doxorubicin clearly played an inhibitory role in lymph node metastases to EMT-6 breast cancer cells.

**MeSH Keywords:** **Breast Neoplasms • Doxorubicin • Drug Therapy, Combination • Lymphatic Metastasis • Nanotubes, Carbon**

**Full-text PDF:** <http://www.medscimonit.com/abstract/index/idArt/898597>

 3169

 2

 8

 30



## Background

There are roughly 1,400,000 women newly diagnosed with breast cancer worldwide every year [1]. Status of axillary lymph nodes is an essential factor affecting the prognosis of breast cancer [2,3]. Surgical dissection of lymph nodes and low proportion of local drug in conventional chemotherapy often results in incomplete treatment, contributing to recurrence as well as metastasis. Lymph nodes, therefore, have become an exceptional potential target organ in cancer chemotherapy.

In the 1970s, Widder first proposed the concept of a magnetic targeted drug delivery system. In the 21<sup>st</sup> century, it has become a novel drug delivery system for treatment of cancer, which is painstakingly researched around the world [4–8]. Using this system, drugs and appropriate magnetically active ingredients are bound in a stable drug system, and carriers are positioned in the target region with the effects of sufficiently strong external magnetic field, and the drugs containing the carriers are positioned and collectively released into the lesion site [9–12]. Presently, the magnetic nanoparticles used in drug carriers consist of magnetic nanoparticles, polymer materials, and therapeutic agents [13]. Carbon nanotubes (CNTs) have attracted tremendous attention due to their unique properties, and are one of the most promising nanomaterials for a variety of biomedical applications [14]. CNTs can be divided into single-walled carbon nanotubes (SWNT) and multi-walled carbon nanotubes (MWNT). In comparison with other nanomaterials, CNTs appear to be more dynamic in their biological application. As a unique quasi one-dimensional material, CNTs have been explored as novel drug delivery vehicles *in vitro*. CNTs can effectively shuttle various biomolecules into cells, including drugs, peptide, proteins, plasmid DNA, and small interfering RNA via endocytosis. The ultrahigh surface area of these one-dimensional polyaromatic macromolecules allows for efficient loading of chemotherapy drugs [15]. Application of CNTs for the delivery of drugs to their site of action has become one of the main areas of interest for different research groups [16–18], mainly because of the characteristics of these materials, including their unique chemical, physical, and biological properties [14]. The nanoneedle shape, hollow monolithic structure, and their ability to obtain the desired functional groups on their outer layers are also very important.

## Material and Methods

### Material

Breast cancer cells of EMT-6 mice were purchased from the Institute of Biochemistry and Cell Biology, SIBS, CAS, Shanghai.

Female BABL/c mice 4–6 weeks old were purchased from the Laboratory Animal Center, Southern Medical University.

Primary reagents MWNT with a diameter of 20–30 nm, a length of 5–15  $\mu\text{m}$ , and a purity of 95% (wt) were purchased from Chengdu Organic Chemicals Co., Ltd. of the Chinese Academy of Sciences (COCC).

### Methods

#### *Preparation and testing of magnetic multi-walled carbon nanotube-doxorubicin*

Preparation for magnetic multi-walled carbon nanotube-doxorubicin (DOX-O-mMWNT-PEG)

With ultrasonication, O-MWNT was produced by concentrated acid oxidation and the number of carboxyl on the surface of MWNT was determined through acid-base titration. To increase solubility and biocompatibility of O-MWNT, O-MWNT and PEG were connected by non-covalent bonds to obtain O-MWNT-PEG. O-mMWNT-PEG was produced by chemically synthesizing  $\text{Fe}_3\text{O}_4$  nanoparticles in O-MWNT-PEG. Magnetic particles were prepared to carry the drugs, and then the magnetic particles bound doxorubicin to generate DOX-O-mMWNT-PEG. Achieved dissolution used a Millipore filter (100 k Da), centrifuged at 5000 rpm for 10 min and washed with deionized water 10 times. The solid at the upper part of the Millipore filter was dissolved with PBS at pH 9.0 to achieve DOX-O-mMWNT-PEG. Unlinked free DOX at the bottom of the Millipore filter was collected for determination of drug loading. The concentration of DOX was determined with ultraviolet visible spectroscopy at 480 nm. Drug loading (DL) was calculated based on the following formula:

$$\text{DL}\% = \frac{\text{Inventory of DOX} - \text{unlinked DOX}}{\text{weight of O - mMWNT - PEG} + (\text{Inventory of DOX} - \text{unlinked DOX})} \times 100\%$$

#### Detection of O-mMWNT-PEG

The morphosis of O-mMWNT-PEG was observed with a transmission electron microscope; the stability and magnetic responsiveness of O-mMWNT-PEG suspension were observed at normal temperature.

#### *Determination of cytotoxicity*

EMT6 murine breast cancer cell line was cultured in the standard medium. Cells were plated in 96-well plates and treated with different concentrations of O-mMWNT-PEG, DOX-O-mMWNT-PEG, or DOX for 3 days. Cell viability after various treatments was assessed by 3-(4, 5-dimethyl thiazol- 2- yl)-2, 5-diphenyltetrazolium bromide.

### Establishment of the lymph node metastatic model of breast cancer

Breast cancer cells of EMT-6 mice in exponential phase (over 95% living cells) were collected and cleaned with 1×PBS 3 times, and resuspended cells were repeatedly pipetted with 1×PBS; the concentration of cells were adjusted to  $1 \times 10^8$  mL<sup>-1</sup>; cell suspension was produced and put on ice of 4°C. Each BABL/c mouse was inoculated with 0.2 ml of such cell suspension to the left foot pad and the formation of tumor and popliteal lymph node metastasis were observed. Five weeks later, those with bean-size lymph nodes on the left popliteal fossa were identified as ideal animal models. Two mice of such models were sacrificed, with their lymph nodes on the left popliteal fossa cut; the nodes were fixed in 10% neutral-buffered formalin. Paraffin sections stained with H&E were viewed with an upright microscope and photographed by DP2-BSW.

### Observation of effectiveness of DOX-O-mMWNT-PEG magnetic targeting in treatment of lymph node metastasis in breast cancer of mice

#### Animal grouping

We randomly divided 42 ideal mouse models into 6 groups after tumor cells inoculation 5 weeks later and each group included 7 mice. Group A (normal saline) received subcutaneous injection using 0.1 ml of normal saline(NS) at the left hind limb; group B (empty O-mMWNT-PEG carrier) received subcutaneous injection using 0.1 ml of O-mMWNT-PEG suspension at the left hind limb; group C (DOX monotherapy) received subcutaneous injection using 0.1 ml of DOX (2 mg/ml) at the left hind limb; group D (DOX-O-mMWNT-PEG of low concentration without magnetic field) received subcutaneous injection each time using 0.1 ml of O-mMWNT-PEG suspension of low concentration (including 2 mg/ml of DOX) at the left hind limb and no permanent magnet was applied to the lymph nodes; group E (DOX-O-mMWNT-PEG of low concentration with magnetic field) received subcutaneous injection each time using 0.1 ml of O-mMWNT-PEG suspension of low concentration (including 2 mg/ml of DOX) at the left hind limb and permanent magnet was applied to the lymph nodes; group F (DOX-O-mMWNT-PEG of high concentration with magnetic field) received subcutaneous injection each time with 0.1 ml of O-mMWNT-PEG suspension of high concentration (including 4 mg/ml of DOX) at the left hind limb and a permanent magnet was applied to the lymph nodes. We made 5-mm skin incision to the lymph nodes on the left popliteal fossa of mice in group E and group F 1 day prior to the treatment, strictly complying with principles of sterile operating, a 5-mm diameter magnet was implanted subcutaneously, and the incision was sutured with 3-0 absorbable surgical stitches.

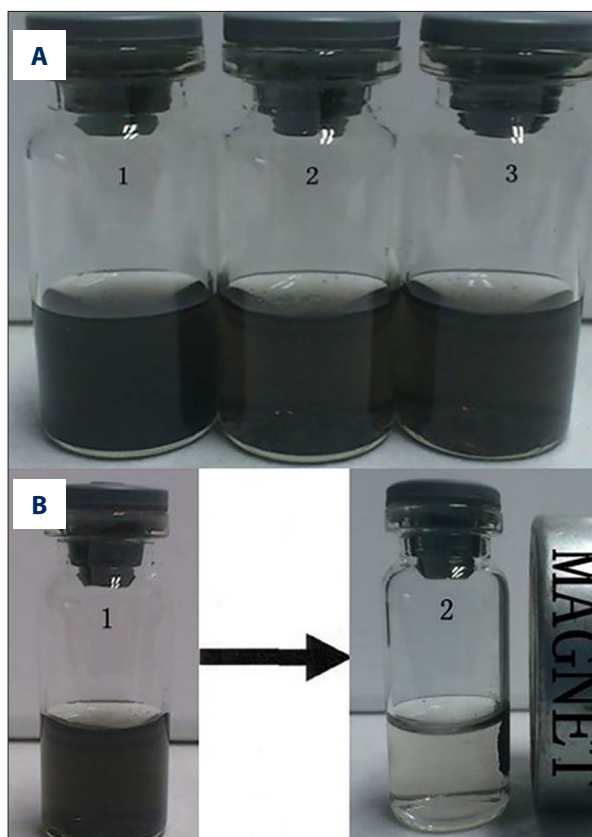


**Figure 1.** The static observation about the O-mMWNT-PEG suspension liquid and the effect caused by magnet attraction. The O-mMWNT-PEG suspension liquid placed for 1 week (a<sub>1</sub>); the O-mMWNT-PEG suspension liquid placed for 2 weeks (a<sub>2</sub>); the O-mMWNT-PEG suspension liquid placed for 1 month (a<sub>3</sub>). Picture B indicates that O-mMWNT-PEG gathered quickly (within 1 min) on the side where the magnet was placed.

#### Observation of effectiveness after subcutaneous injection

The weight of mice and the maximum and minimum diameters of their tumors were recorded on the first day of the sixth week. All groups were administered on the first day of the sixth week and the seventh week, the weight of mice and the maximum and minimum diameters of their tumors were further recorded on the first day of the ninth week, and the changes of weight and tumor volume after the treatment were observed. Tumor volume was calculated based on the formula [19]:  $TV = 1/2 \times D_{max} \times (D_{min})^2$ . Blood of mice was collected from the orbital sinus. WBC, ALT, and Scr tests were run on the first day of the ninth week. Mice were euthanized by cervical dislocation, lymph nodes on the left popliteal fossa of all groups were taken, and the volume of lymph nodes and tumor were calculated based on the formula above; the lymph node growth inhibition rate was calculated (lymph node tumor=(1-average volume of the treatment group/average volume of the control group)×100%); lymph nodes of all groups were weighed and

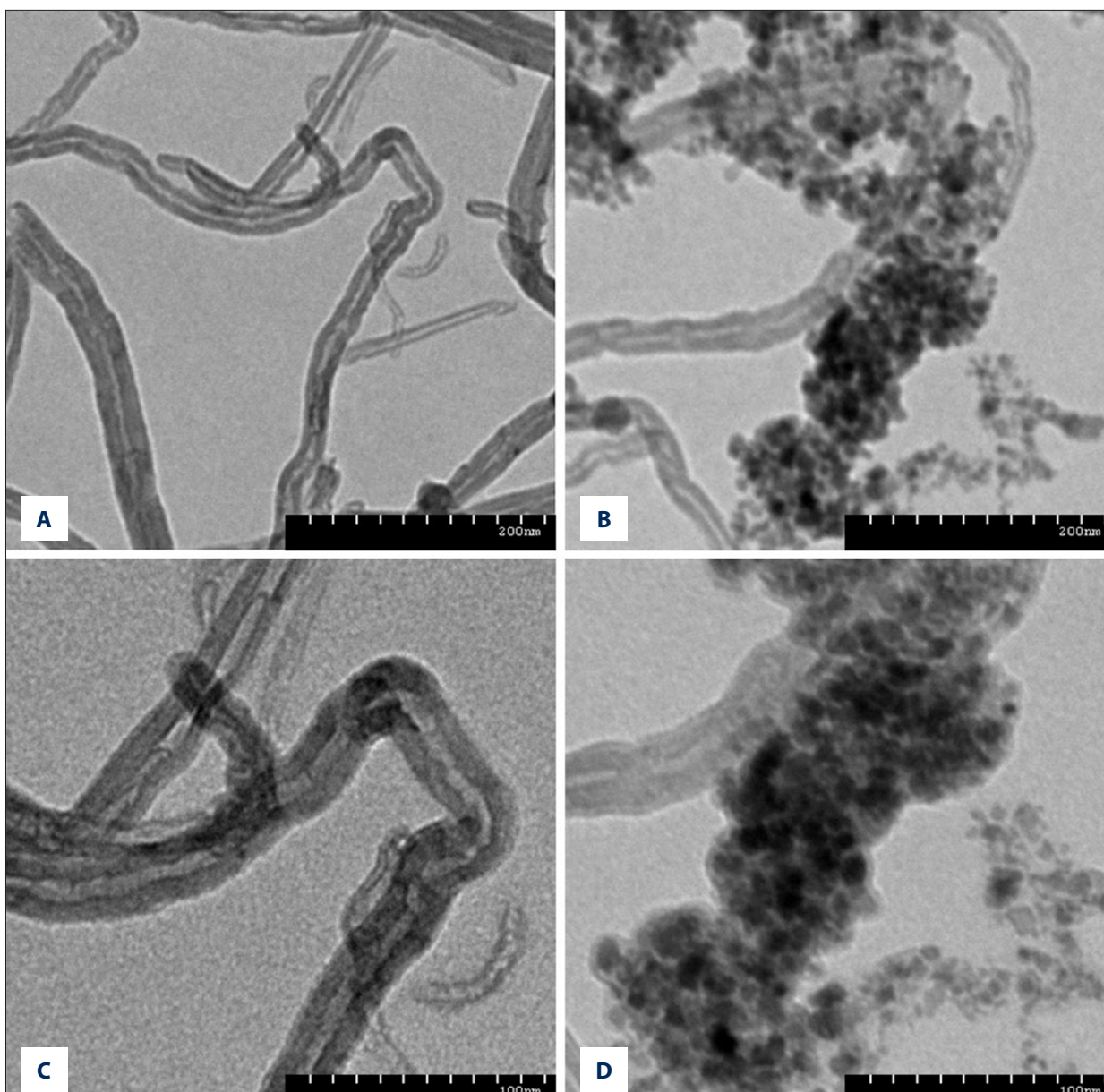


**Figure 2.** The MWNT and O-mMWNT-PEG under the TEM. MWNT without the modification of  $\text{Fe}_3\text{O}_4$  (**A, C**) and MWNT with the modification of  $\text{Fe}_3\text{O}_4$  (**B, D**). There were evenly distributed black particles –  $\text{Fe}_3\text{O}_4$  – settled and absorbed onto the surface of the hollow MWNT tubes.

the lymph nodes mass inhibition rate was calculated (lymph node mass inhibition rate =  $(1 - \text{average mass of the treatment group} / \text{average mass of the control group}) \times 100\%$ ). The skin of the left hind footpad of mice and any signs of anaphylaxis were observed. Histopathological abnormality of important visceral organs, including heart, liver, spleen, lung, and kidney, were observed.

Routine pathological examination of lymph nodes and tumor and detection of cancer cell apoptosis

Tumors of all groups and popliteal lymph nodes were fixed in 10% formalin. Paraffin sections stained with H&E were viewed with an upright microscope. Cancer cell apoptosis of lymph nodes was detected through TDT-mediated DUTP nick-end labeling (TUNEL). Apoptotic index (AI) refers to the number of positive cells counted in 10 HPF successively through a normal light microscope, and then converted to an average number of apoptotic cells in every square millimeter.

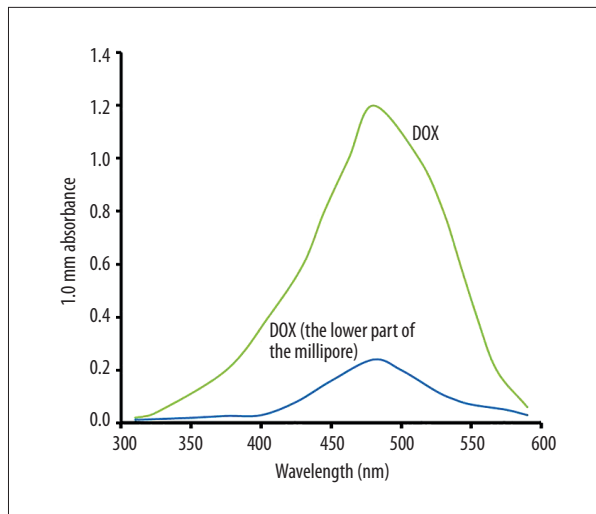


**Figure 3.** The absorption value of the DOX under the UV-Vis-NIR. This figure indicates the absorption peak of the DOX was at 480 nm and DOX conjugated by O-mMWNT-PEG accounted for 80% of the DOX total dose.

### Statistical analysis

Quantitative data are expressed as mean $\pm$ SD. Methods were compared by using the *t* test. *P* values of <0.05 were considered statistically significant.

## Results

### The detection of O-mMWNT-PEG and measurement of its drug loading capacity

O-mMWNT-PEG suspension was black, slightly viscous, and evenly dispersed. The suspension was quite stable under normal temperature. The particles settled slowly and began to form sediments after 2 weeks, but only a few sediments were eventually formed at 1 month. Such sediments were restored to their former characters after being dispersed by ultrasonication at 40 kHz for 2 min (Figure 1); or, after being centrifuged for 15 min and then dispersed by ultrasonication, they were also restored to their former characters. When a magnet was placed near a bottle of O-mMWNT-PEG suspension, O-mMWNT-PEG gathered quickly on the side where the magnet was placed within 1 min (Photograph 1). When examined under a transmission electron microscope (TEM), it could be seen that the O-MWNT-PEG without the modification of Fe<sub>3</sub>O<sub>4</sub> were in the form of long tubes that have a transparent core and opaque walls, about 40 nm in diameter and 1–2  $\mu$ m long, with few impurities and a smooth surface (Figure 2). After the modification of Fe<sub>3</sub>O<sub>4</sub> nanoparticles, the black Fe<sub>3</sub>O<sub>4</sub> particles settled and were absorbed onto the surface of the hollow O-MWNT-PEG tubes and were evenly distributed, although some

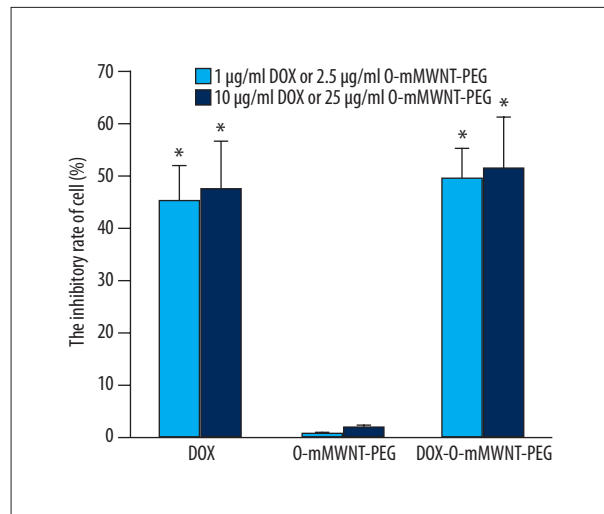


**Figure 4.** The inhibition ratio to the EMT-6 cell from different groups of medicines. \* *P*<0.01 vs. both group of O-mMWNT-PEG.

gathered at certain places (Figure 2). When 20 ml of DOX was dissolved in 20 ml PBS at pH 9.0, we could see from the curve (Figure 3) drawn based on the results obtained from UV-Vis-NIR spectrophotometer at 480 nm. The solution was washed with a Millipore filter 10 times and then 20 ml of reddish liquid was collected at the bottom of the filter. Since O-mMWNT-PEG conjugated with DOX are 200 nm in diameter, they could not pass through the mesh screen. Therefore, the collected liquids were O-mMWNT-PEG with non-conjugated DOX. The concentration of DOX measured through ultraviolet spectroscopy and its DL was 80% based on calculation (0.8 mg/ml).

### The measurement of cytotoxicity

To determine the cytotoxicity on EMT-6 *in vitro*, PBS was used in the negative control group, with a series of DOX, O-mMWNT-PEG, and DOX-O-mMWNT-PEG solutions of different concentrations as experimental groups. The results of MTT assay showed that the cytotoxicity of O-mMWNT-PEG to EMT-6 breast cancer cells was quite low even when the concentration was up to 10  $\mu$ g/ml, which was significantly different from other groups (*P*<0.01) (Figure 4). The inhibitory effects of DOX on breast cancer cells depended on its concentration; when O-mMWNT-PEG was added, the inhibition rate increased slightly, yet without statistical difference (*P*>0.05) (Figure 4). The inhibitory effects of DOX and DOX-O-mMWNT-PEG with the same concentration of DOX on EMT-6 breast cancer cells were not significant. All these results show that the pharmaceutical activity of DOX was not affected during the preparation of DOX-O-mMWNT-PEG and the main component that had inhibitory effects on EMT-6 breast cancer cells *in vitro* was DOX.

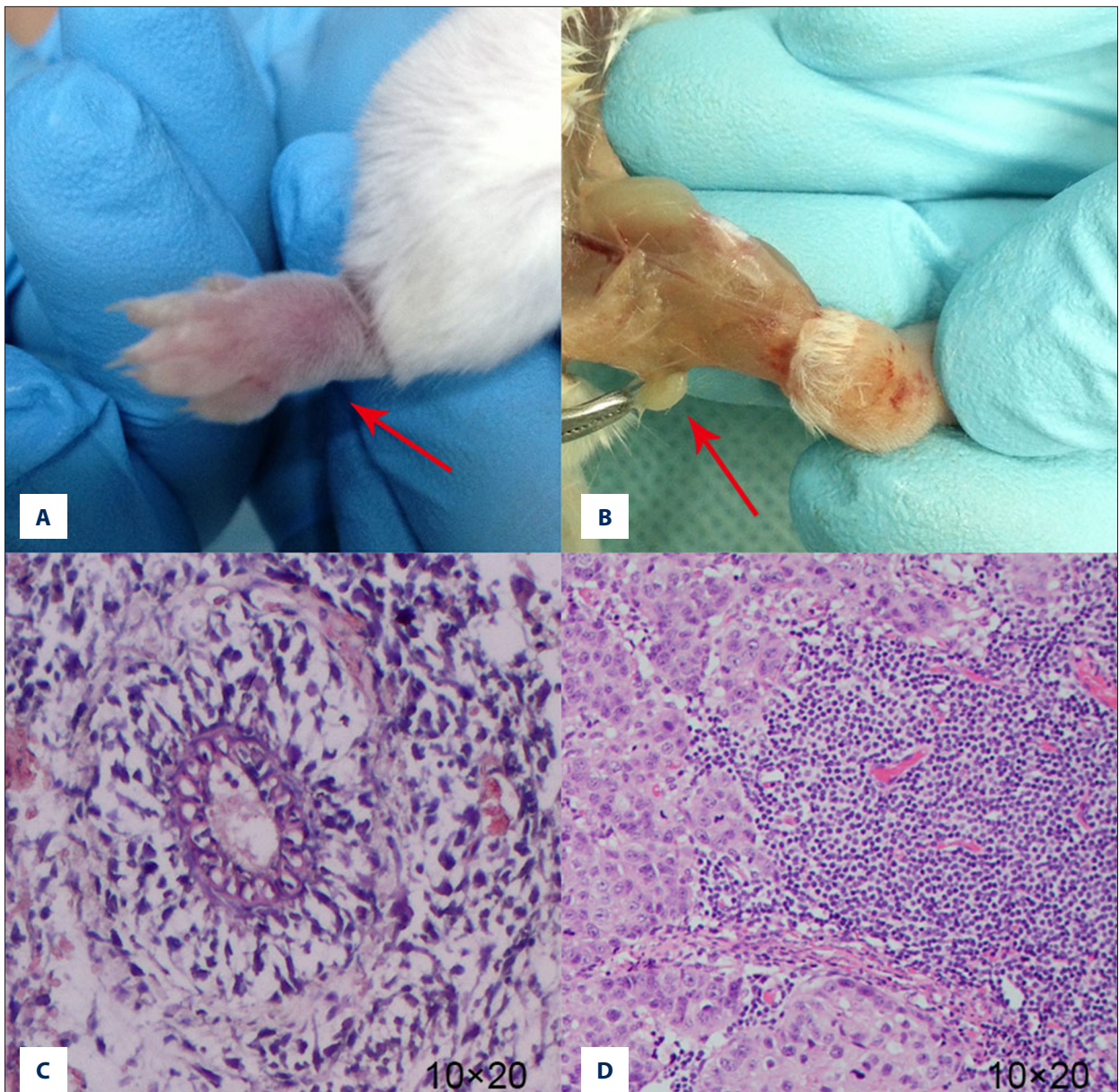


**Figure 5.** The general samples and HE staining of transplanted tumor and metastatic lymph node. The red arrows show the general samples of the transplanted tumor and the metastatic lymph node, respectively (A, B). Photograph C and D show the HE staining (10×20) of the transplanted tumor and the metastatic lymph node, respectively. We found cancer cells of different sizes and shapes. Such cells were deformed, mostly in the shape of a nest, glandular tube, or in disorder (C, D).

#### Determination of animal model of breast cancer in mice

The tumor formation rate on the footpads of the mice was 90% after inoculation with EMT-6 cells (Figure 5). The metastatic lymph node of the popliteal fossa is shown in Figure 2. Under a microscope, it could be seen that the cells of the tumor tissue were of different sizes and shapes, with large and hyperchromatic nuclei. Such cells were deformed, in the shape of a nest, glandular tube, or in disorder, and some of them were necrotic (Figure 5). The results of pathological examination of lymph

nodes metastasis showed that the cancer cells were scattered or developed into small metastatic carcinoma.

#### Observation on effectiveness of DOX-O-mMWNT-PEG magnetic targeting treatment for lymph node metastases in breast cancer of mice

In the process of treatment, no mice died. Table 1 shows the changes in the weight of mice and the size of the tumors before and at 2 weeks after the drugs were administered, showing

**Table 1.** The comparison of the weight, the volume of the tumor from the mice before and after given the medicine as well as the weight and the volume of the popliteal lymph node.

Group	Before administration		After administration		Lymph nodes on the popliteal fossa	
	Weight of the mice (g)	Tumor volume (mm <sup>3</sup> )	Weight of the mice (g)	Tumor volume (mm <sup>3</sup> )	Mass (g)	Volume (mm <sup>3</sup> )
A	24.14±1.22	107.21±38.31	24.71±1.80	205.29±61.1	21.73±6.20	23.11±7.21
B	23.00±1.16	103.71±26.58	23.71±1.60	214.71±61.25	31.71±8.06 <sup>#</sup>	32.74±7.45 <sup>**</sup>
C	23.43±1.62	108.00±42.40	24.14±1.46	168.71±48.58 <sup>*</sup>	20.40±8.06 <sup>&amp;</sup>	22.20±7.66 <sup>##</sup>
D	23.29±1.38	89.86±21.43	23.86±1.57	144.86±30.25 <sup>*</sup>	15.64±5.23 <sup>&amp;</sup>	18.49±5.23 <sup>**##</sup>
E	24.14±1.57	101.57±41.5	24.71±1.50	152.43±58.89 <sup>*</sup>	9.57±3.46 <sup>#, &amp;, @</sup>	11.07±3.32 <sup>**##, &amp;, &amp;</sup>
F	23.29±1.80	102.57±28.75	24.14±1.54	158.86±33.35 <sup>*</sup>	12.83±4.61 <sup>#, &amp;, @</sup>	11.14±4.49 <sup>**##, &amp;, &amp;</sup>

\* Is comparison between Group C, D, E, F and Group A, B, P<0.05, # is comparison between Group B, E, F and Group A, P<0.05; & is comparison between Group C, D, E, F and Group B, P<0.05; @ is comparison between Group E, F and Group C, D, P<0.05. \*\* Is comparison between Group B, E, F and Group A, P<0.05; ## is comparison between Group C, D, E, F and Group B, P<0.05; && is comparison between Group E, F and Group C, P<0.05.

**Table 2.** The comparison of blood routine and biochemical criterion among the mice from each groups.

Group	WBC (×10 <sup>9</sup> /L)	RBC (×10 <sup>9</sup> /L)	HB (g/L)	PLT (×10 <sup>9</sup> /L)	ALT (U/L)	Scr (μmol/L)
A	8.81±1.80	9.66±0.86	13.2±7.0	208.2±118.1	60.2±14.8	33.8±2.3
B	9.1±2.43	10.25±0.39	17.1±0.6	157.6±29.3	63.1±10.5	33.1±4.5
C	3.31±1.26 <sup>*</sup>	9.89±0.74	16.4±1.7	185.0±102.9	73.4±18.3	30.1±8.7
D	4.35±1.35	9.32±2.44	14.5±6.3	157.6±100.1	65.1±15.7	34.0±3.3
E	5.15±1.51	9.83±1.26	14.9±4.7	199.1±71.7	63.7±19.1	33.8±3.5
F	4.16±1.68	9.80±1.01	14.5±5.9	156.3±87.0	66.1±18.2	34.5±8.2

\* P<0.05 vs. group A and B.

that the weight of the mice did not change significantly. After treatment, comparing group C, D, E, and F with group A and B, the tumors from the former groups were obviously smaller than in group A and B. However, there was no distinct difference between these 4 groups. We collected blood from the orbital sinus and performed WBC, ALT, and Scr tests. As indicated in Table 2, the level of WBC decreased in the DOX group but the indicators of the mice in other groups were normal. The mice were sacrificed on the first day of the ninth week and the lymph nodes on the left popliteal fossa were taken out to measure the weight of the lymph nodes and calculate their volume based on the formula (Table 1, Figure 6). The weight and volume of the lymph nodes of the blank carrier group and the control group increased slightly, perhaps because the magnetic multi-walled carbon nanotube in the lymph nodes led to increased weight and volume. With outside magnetic field, the volume and weight of the lymph nodes carrying DOX-O-mMWNT-PEG was reduced, and with the increasing of the dose of DOX, they reduced more. Apoptotic cells with

claybank or brown nuclei in the tumors could be detected via TUNEL method (Figure 7). From the apoptosis index shown in Figure 7, the apoptosis rate of the cancer cells in the lymph nodes in group A was the lowest and there was a significant difference (P<0.05) between these groups, except for group B. The apoptosis rate of Group E and F were obviously higher than that of Group C (P<0.05). The apoptosis rate of Group F was obviously higher than that of Group D (P<0.05). No statistical significance was shown between Group E and F (P>0.05). The injection sites at left hind limbs of the mice were stained black after the injection of drugs, but there was no redness, swelling, ulceration, or corrosion (Figure 8). The mice did not have allergy, nausea, or emesis, and they appeared normal. Histopathological examination showed that no multi-walled carbon nanotube particles gathered in important viscera such as the heart, liver, spleen, lung, or kidney, and no pathologic changes like inflammation, fibrosis, or granuloma occurred in these organs (Figure 8).

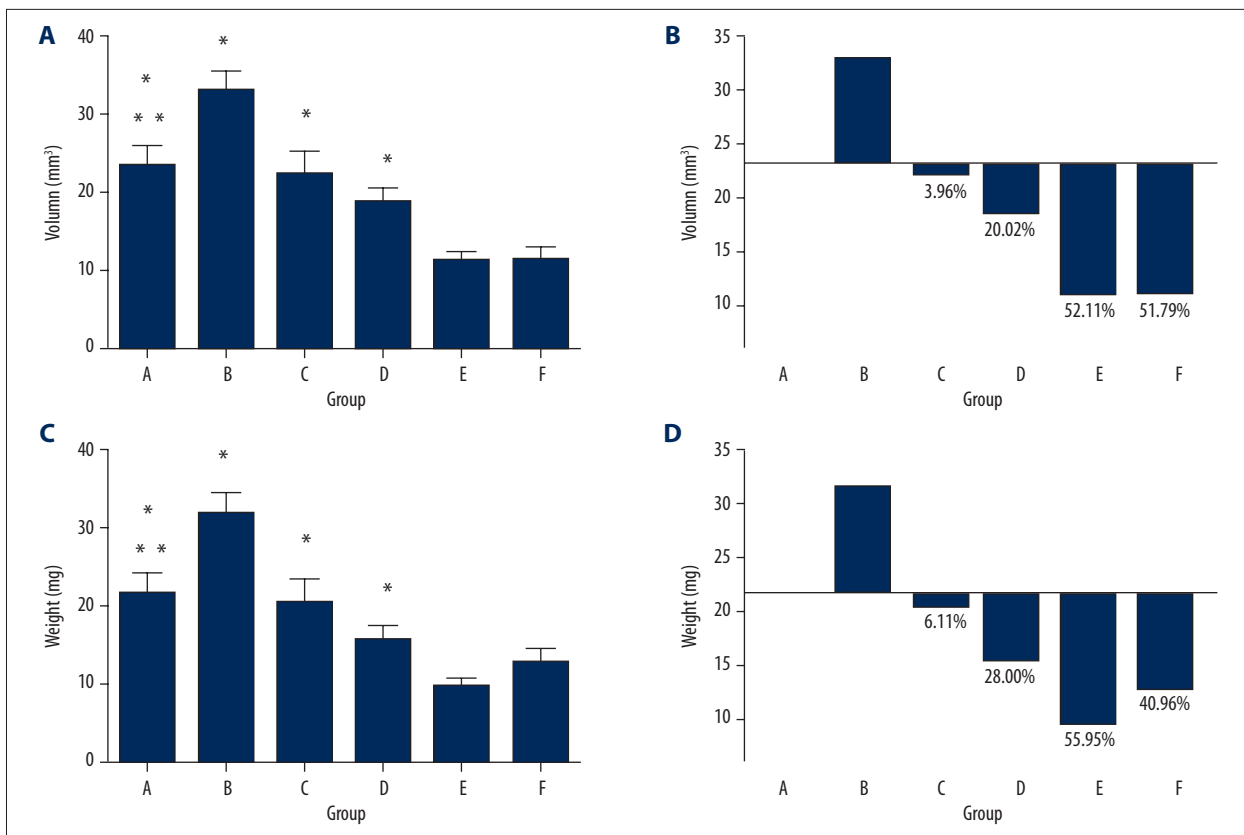


**Figure 6.** (A–D) The distribution and the inhibition ratio of the weight and volume of lymph node in each group. \*  $P < 0.05$  vs. group E, F, \*\*  $P < 0.05$  vs. group B. Figure B and D used the volume and the weight of the lymph nodes of group A as baseline. Over the x axis, the positive half refers to the increases of the volume and the weight, while the other half refers to the inhibition of the weight and the volume. The number equals the inhibition ratio.

## Discussion

Experiments *in vitro* indicated that the O-mMWNT targeted drug delivery system was effective in inhibiting the growth of breast cancer EMT6 cells. Experiments *in vivo* showed that O-mMWNT gathered around lymph nodes and the tumors, releasing drugs continuously for a long span of time, inhibiting the growth of breast cancer cells and lymph nodes metastasis. Yang et al. [20,21] conducted an animal study using O-mMWNT as a carrier for Gemcitabine in pancreatic cancer lymphatic chemotherapy. These studies also indicated that O-mMWNT entered the lymphatic channel, gathering towards external magnetic field targeting lymph nodes, and releasing chemotherapeutic drugs continuously for a long span of time. Liu et al. [22] used mMWNT as a carrier for Paclitaxel through conjugation, and conducted experiments in a mouse breast cancer model. These experiments indicated that MWNT could improve drug concentration in blood and around tumors. DOX-O-mMWNT-PEG had inhibitory effects on lymph node metastasis and the growth of breast tumors. To a certain extent, the volume and mass of metastatic lymph nodes indicate the degree of lymph nodes metastasis, but there are

many other influencing factors. This study showed that the volume and mass of lymph nodes and tumor of Group B were slightly larger than those of Group A, which probably was a result of the entry of carriers. The volume and mass of lymph nodes of Group E and F were reduced in the magnetic fields, and reduced more as the amount of drugs used increased, which demonstrates that O-mMWNT plays an important role in targeting lymph nodes and tumors. Apoptosis is a measurement of the effectiveness of tumor treatment [23]. In this study, we used TUNEL to detect apoptosis in lymph nodes and tumors to calculate the apoptosis index. Results showed that DOX and magnetic particles conjugate had stronger inhibitory effects on tumors of mice and lymph node metastasis than simply using DOX. Moreover, antitumor effects were more significant under the influence of the magnetic field. This conjugate, 1-1000 nm in diameter, is a type of carrier in targeting treatment. With the assistance of a magnetic field, the drug carriers gather around the targeted sites and steadily release the drugs so that drug concentration at the targets can be increased and the effectiveness enhanced. Drugs in other sites can be reduced and thus the toxicity and adverse effects will be lower. According to other reports, this drug carrier can also

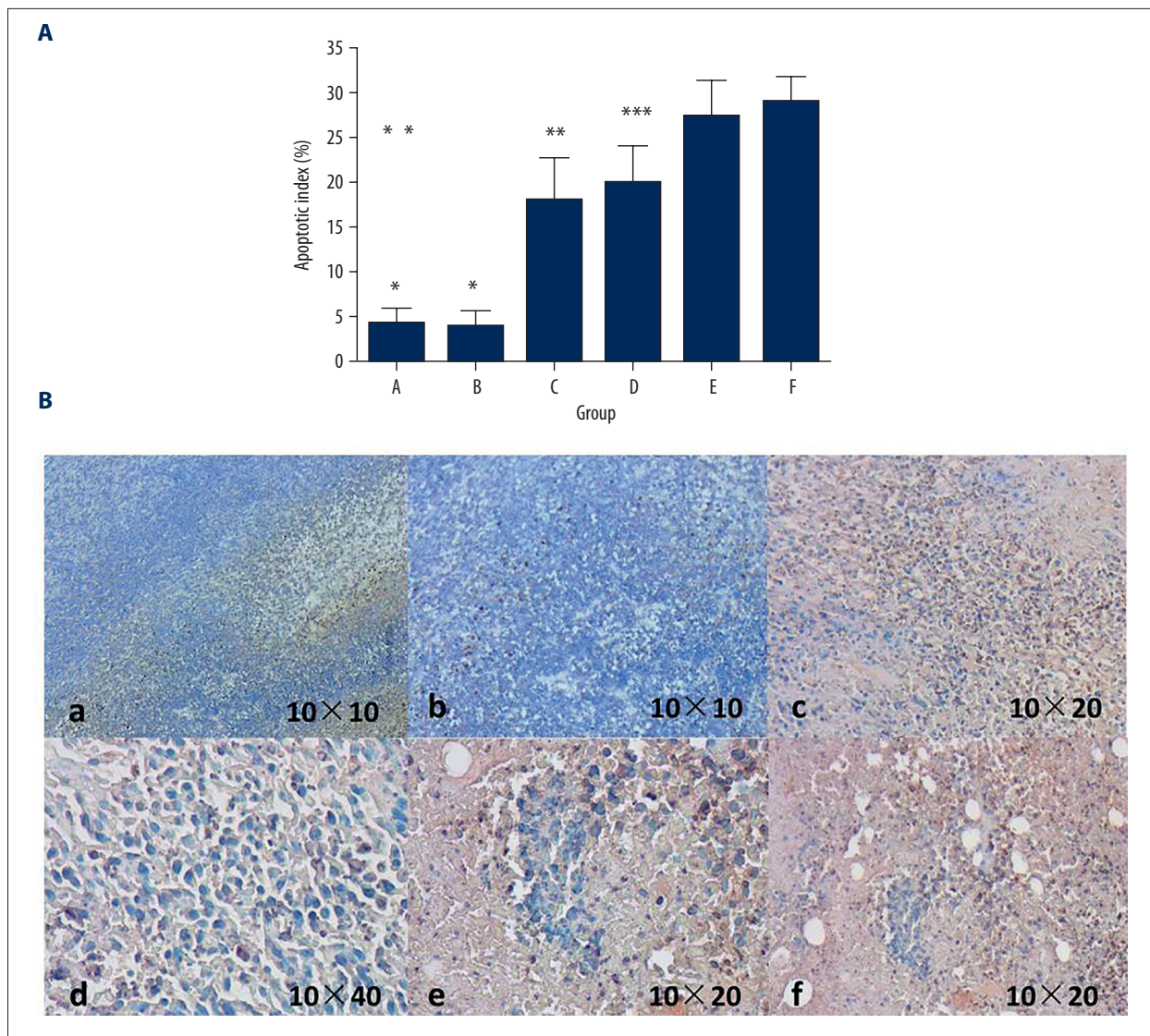


**Figure 7.** Tumor cell apoptosis of the popliteal lymph nodes. \*  $P < 0.05$  vs. group C, D, E, F, \*\*  $P < 0.05$  vs. group E, F, \*\*\*  $P < 0.05$  vs. group F. In picture **B**, cells, which nuclear stained in yellow or brown, were the tumor apoptotic cells.

be used in thermal therapy [24,25], in which, with the assistance of fixed magnetic field and alternating magnetic field, it can kill or injure the cancer cells with the heat generated by magnetic lag [26]. WBC results indicated that chemotherapy targeting lymph nodes has few adverse effects. This conclusion is consistent with relevant studies [20,21].

Studies also showed that magnetic carbon nanotubes can easily identify blackened lymph nodes during operations, indicating better tracing effect during operations. Pramanik et al. [27] detected sentinel nodes of mice with breast cancer through photoacoustic imaging improved by carbon nanotubes, showing the satisfactory effect of identification. Our experiment also suggested good performance of mMWNT in tracing lymph, and even tiny lymph nodes with diameter of 1–2 mm could be

blackened. The carrier of mMWNT could reach the next lymph node even when there was metastasis within this lymph node. In clinical studies, it is effective and safe to apply methylene blue to locating sentinel nodes of tumors [28,29], but Kocher et al. [30], using methylene blue as a lymph tracer to study sentinel nodes of pancreatic cancer, found that no metastasis occurred among 4 patients with stained lymph, while metastasis was detected among all 10 patients with unstained lymph. The reasons might lie in preparations, injection sites, anatomical structures, and characteristics of tumors. Both carriers we prepared showed good lymph taxis, adding a choice in studies on sentinel node of pancreatic cancer.

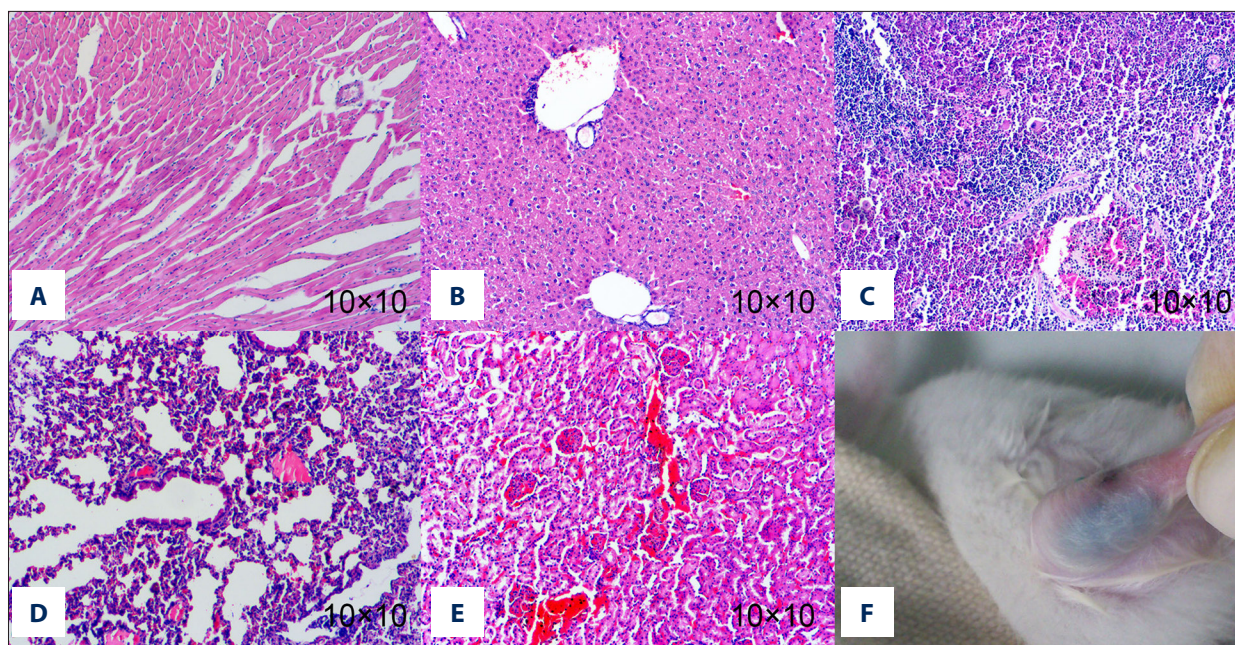


**Figure 8.** The pathological section from the organs of mice and the general observation of the injected part. There was no gathering of multi-walled carbon nanotube particles in heart, liver, spleen, lung, or kidney of the mice, or pathological changes such as inflammation, fibrosis, or granuloma in these such organs (A–E). The injection site showed no redness, swelling, ulceration, or corrosion (F).

## Conclusions

O-mMWNT is a novel targeted drug delivery carrier with features of lymph taxis and magnetic targeting administration. We used O-mMWNT -DOX to study lymph metastasis while conducting experimental studies of magnetic targeting treatment. Our encouraging results may provide an experimental

basis for application of new materials, new dosage forms, and new methods to treat lymph metastasis of tumors, reducing adverse effects and improving cure rates throughout the body.

## Conflict of interest

There is no conflict of interest.

## References:

- Jemal A, Center MM, DeSantis C, Ward EM: Global patterns of cancer incidence and mortality rates and trends. *Cancer Epidemiol Biomarkers Prev*, 2010; 19: 1893–907
- Wu JL, Tseng HS, Yang LH et al: Prediction of axillary lymph node metastases in breast cancer patients based on pathologic information of the primary tumor. *Med Sci Monit*, 2014; 20: 577–81
- Tseng HS, Chen LS, Kuo SJ et al: Tumor characteristics of breast cancer in predicting axillary lymph node metastasis. *Med Sci Monit*, 2014; 20: 1155–61
- Yang F, Jin C, Yang D et al: Magnetic functionalised carbon nanotubes as drug vehicles for cancer lymph node metastasis treatment. *Eur J Cancer*, 2011; 47: 1873–82
- Razzazan A, Atyabi F, Kazemi B, Dinarvand R: *In vivo* drug delivery of gemcitabine with PEGylated single-walled carbon nanotubes. *Mater Sci Eng C Mater Biol Appl*, 2016; 62: 614–25
- Melita ED, Purcel G, Grumezescu AM: Carbon nanotubes for cancer therapy and neurodegenerative diseases. *Rom J Morphol Embryol*, 2015; 56: 349–56
- Dineshkumar B, Krishnakumar K, Bhatt AR et al: Single-walled and multi-walled carbon nanotubes based drug delivery system: Cancer therapy: A review. *Indian J Cancer*, 2015; 52: 262–64
- Ou Z, Wu B: A novel nanoprobe based on single-walled carbon nanotubes/ photosensitizer for cancer cell imaging and therapy. *J Nanosci Nanotechnol*, 2013; 13: 1212–16
- Qi X, Rui Y, Fan Y et al: Galactosylated chitosan-grafted multiwall carbon nanotubes for pH-dependent sustained release and hepatic tumor-targeted delivery of doxorubicin *in vivo*. *Colloids Surf B Biointerfaces*, 2015; 133: 314–22
- Dong X, Liu L, Zhu D et al: Transactivator of transcription (TAT) peptide-chitosan functionalized multiwalled carbon nanotubes as a potential drug delivery vehicle for cancer therapy. *Int J Nanomedicine*, 2015; 10: 3829–40
- Neves LF, Kraiss JJ, Van Rite BD et al: Targeting single-walled carbon nanotubes for the treatment of breast cancer using photothermal therapy. *Nanotechnology*, 2013; 24: 375104
- Das M, Singh RP, Datir SR, Jain S: Intracellular drug delivery and effective *in vivo* cancer therapy via estradiol-PEG-appended multiwalled carbon nanotubes. *Mol Pharm*, 2013; 10: 3404–16
- Al FA, Shaik AP, Shaik AS: Magnetic single-walled carbon nanotubes as efficient drug delivery nanocarriers in breast cancer murine model: Noninvasive monitoring using diffusion-weighted magnetic resonance imaging as sensitive imaging biomarker. *Int J Nanomedicine*, 2015; 10: 157–68
- Sahoo NG, Bao H, Pan Y et al: Functionalized carbon nanomaterials as nanocarriers for loading and delivery of a poorly water-soluble anticancer drug: A comparative study. *Chem Commun (Camb)*, 2011; 47: 5235–37
- Liu Z, Sun X, Nakayama-Ratchford N, Dai H: Supramolecular chemistry on water-soluble carbon nanotubes for drug loading and delivery. *ACS Nano*, 2007; 1: 50–56

16. Chen C, Zhang H, Hou L et al: Single-walled carbon nanotubes mediated neovascularity targeted antitumor drug delivery system. *J Pharm Pharm Sci*, 2013; 16: 40–51
17. Das M, Singh RP, Datir SR, Jain S: Intracellular drug delivery and effective *in vivo* cancer therapy via estradiol-PEG-appended multiwalled carbon nanotubes. *Mol Pharm*, 2013; 10: 3404–16
18. Elhissi AM, Ahmed W, Hassan IU et al: Carbon nanotubes in cancer therapy and drug delivery. *J Drug Deliv*, 2012; 2012: 837327
19. Ogawa K, Mukai T, Asano D et al: Therapeutic effects of a <sup>186</sup>Re-complex-conjugated bisphosphonate for the palliation of metastatic bone pain in an animal model. *J Nucl Med*, 2007; 48: 122–27
20. Yang F, Hu J, Yang D et al: Pilot study of targeting magnetic carbon nanotubes to lymph nodes. *Nanomedicine (Lond)*, 2009; 4: 317–30
21. Yang F, Jin C, Jiang Y et al: Liposome based delivery systems in pancreatic cancer treatment: from bench to bedside. *Cancer Treat Rev*, 2011; 37: 633–42
22. Liu Z, Chen K, Davis C et al: Drug delivery with carbon nanotubes for *in vivo* cancer treatment. *Cancer Res*, 2008; 68: 6652–60
23. Kerr JF, Winterford CM, Harmon BV: Apoptosis. Its significance in cancer and cancer therapy. *Cancer*, 1994; 73: 2013–26
24. Hamaguchi S, Tohnai I, Ito A et al: Selective hyperthermia using magnetoliposomes to target cervical lymph node metastasis in a rabbit tongue tumor model. *Cancer Sci*, 2003; 94: 834–39
25. Viroonchatapan E, Ueno M, Sato H et al: Preparation and characterization of dextran magnetite-incorporated thermosensitive liposomes: An on-line flow system for quantifying magnetic responsiveness. *Pharm Res*, 1995; 12: 1176–83
26. Shinkai M, Ito A: Functional magnetic particles for medical application. *Adv Biochem Eng Biotechnol*, 2004; 91: 191–220
27. Pramanik M, Song KH, Swierczewska M et al: *In vivo* carbon nanotube-enhanced non-invasive photoacoustic mapping of the sentinel lymph node. *Phys Med Biol*, 2009; 54: 3291–301
28. Varghese P, Abdel-Rahman AT, Akberali S et al: Methylene blue dye – a safe and effective alternative for sentinel lymph node localization. *Breast J*, 2008; 14: 61–67
29. Yuan SH, Xiong Y, Wei M et al: Sentinel lymph node detection using methylene blue in patients with early stage cervical cancer. *Gynecol Oncol*, 2007; 106: 147–52
30. Kocher HM, Sohail M, Benjamin IS, Patel AG: Technical limitations of lymph node mapping in pancreatic cancer. *Eur J Surg Oncol*, 2007; 33: 887–91